DOI: 10.1002/anie.201200351

Renewable Resources

Tungsten Trioxide Promoted Selective Conversion of Cellulose into Propylene Glycol and Ethylene Glycol on a Ruthenium Catalyst**

*Yue Liu, Chen Luo, and Haichao Liu**

Cellulose is the most abundant source of biomass and has received considerable attention as a vitally renewable alternative to fossil fuels.[1–3] Consequently, different primary routes for the conversion of cellulose with potentially high energy efficiency and atom economy have been explored.[1,3–9] As such, catalytic conversion of cellulose to polyols is particularly noteworthy because of the versatile uses of polyols as chemicals directly and as precursors in the synthesis of fuels and value-added compounds.[1,4d,10,11]

Conversion of cellulose to polyols involves hydrolysis of cellulose by inorganic acids to glucose, and subsequent hydrogenation of glucose to sorbitol and other polyols.[4d,f–h] For example, recent studies showed that combination of water-soluble heteropoly acids and Ru/C catalysts is efficient for cellulose conversion to hexitols (sorbitol and mannitol).[4f,g] Fukuoka and Dhepe reported the direct conversion of cellulose to hexitols on Pt/Al_2O_3 in water without use of any mineral acids.[5a] Following this pioneering work, we developed a more efficient approach by combining hydrolysis with H^+ ions, which are reversibly formed in situ in hot water, with instantaneous hydrogenation on Ru/C.[6a] This green approach has recently been further studied, for example, by replacing Ru/C with different catalysts, such as carbon nanotube supported Ru,[8a] carbon nanofiber supported nickel,[9] and activated carbon supported nickel phosphide,[7c] leading to improved yields of hexitols. More noticeably, Ji et al. achieved the direct conversion of cellulose to ethylene glycol with high yields (e.g., ≈60%) on supported tungsten carbide catalysts (e.g., Ni–W_2C/C).[7a,b] Although the active sites of the carbides and the underlying mechanism of the C–C bond cleavage remain unclear, this work provides a novel route to the sustainable synthesis of ethylene glycol, an important commodity chemical that is currently dependant on petroleum-derived ethylene as precursor. These progresses demonstrate the feasibility of the rational control of the polyol distributions by exploring effective catalytic systems for the hydrolysis of cellulose and subsequent reactions of the sugar intermediates under mild conditions.

Herein, we report an efficient conversion of cellulose into ethylene glycol, propylene glycol, or sorbitol as dominant products on Ru/C in the presence of WO_3 (Scheme 1).

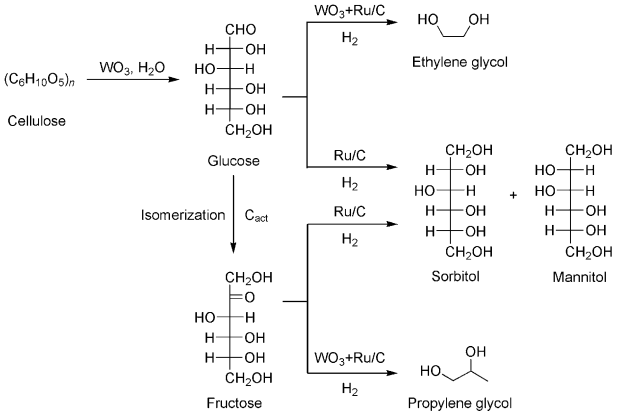

Scheme 1. Catalytic conversion of cellulose into polyols.

Depending on the domain size of WO_3, as a solid acid it promotes not only the hydrolysis of cellulose to sugars (e.g., glucose), but also the selective cleavage of the C–C bonds in the sugar intermediates, thus leading to the preferential formation of ethylene glycol and propylene glycol (Scheme 1). In particular, propylene glycol, an important commodity chemical like ethylene glycol, can be obtained directly from cellulose with an unprecedented yield (>30%).

Table 1 shows the cellulose conversions and selectivities on Ru/C in hot water both in the presence and absence of WO_3. The effects of WO_3 on the product selectivities were examined mostly at similar cellulose conversions of approximately 20%. At 478 K and 6 MPa H_2, cellulose conversion was 12.5% after 30 minutes in the absence of WO_3, and the major product was sorbitol with a selectivity of 54.4% (Table 1, entry 1), as reported previously.[6a] Combined with mannitol (10.3%), the total selectivity to hexitols was 64.7%. Other products included ethylene glycol (7.5%), propylene glycol (3.3%), glycerol (3.0%). After addition of bulk WO_3, cellulose conversion increased from 12.5% to 23.4% (Table 1, entry 2), as a result of the acidity of WO_3.[12] Notably, the product distribution changed; the selectivity to ethylene glycol increased dramatically from 7.5% to 51.5%, concurrently with the decline of the selectivity to hexitols from 64.7% to 16.9% (15.0% sorbitol and 1.9% mannitol). These results clearly show the bifunctional role of WO_3 in accelerating the cellulose hydrolysis and C–C bond cleavage. Upon addition of activated carbon (C_{act}) physically mixed with WO_3, the cellulose conversion remained essentially

[*] Y. Liu, C. Luo, Prof. Dr. H. Liu
Beijing National Laboratory for Molecular Sciences, State Key Laboratory for Structural Chemistry of Stable and Unstable Species, College of Chemistry and Molecular Engineering, Peking University
Beijing 100871 (China)
E-mail: hcliu@pku.edu.cn

[**] This work was supported by the National Natural Science Foundation of China (Grants 20825310, 21173008, and 51121091) and the National Basic Research Project of China (Grants 2011CB808700 and 2011CB201400).

Supporting information for this article is available on the WWW under http://dx.doi.org/10.1002/anie.201200351.

Table 1: Conversion and selectivity in cellulose reaction on Ru/C.[a]

Entry	Catalyst[b]	Conversion [%]	Selectivity [%]						
			Ethylene glycol C_2	Propylene glycol C_3	Glycerol C_3	Tetritols[c] C_4	Pentitols[d] C_5	Mannitol C_6	Sorbitol C_6
1	–	12.5	7.5	3.3	3.0	3.2	10.3	10.3	54.4
2	WO_3	23.4	51.5	6.7	2.8	3.8	1.1	1.9	15.0
3	$WO_3 + C_{act}$	22.8	24.4	31.9	6.7	2.5	0.4	1.4	6.7
4	C_{act}	14.2	6.2	6.7	4.0	2.2	6.7	6.7	52.1
5	0.5 %WO_3/C	20.1	25.7	37.6	5.1	1.3	0	0.6	2.5
6	12 %WO_3/ZrO_2	18.5	11.5	4.0	3.9	1.3	4.6	5.1	58.3
7	50 %WO_3/ZrO_2	20.1	34.9	6.5	3.6	7.3	1.8	5.3	26.1
8	12 %WO_3/TiO_2	18.0	10.2	4.6	2.1	2.3	9.1	9.5	60.5
9	36 %WO_3/TiO_2	20.0	37.5	8.5	3.6	7.2	1.4	4.4	25.3
10	12 %WO_3/Al_2O_3	16.1	25.5	10.6	7.5	4.8	2.5	5.9	37.5
11	50 %WO_3/Al_2O_3	21.5	45.0	10.0	5.2	6.0	0.7	3.0	13.8
12	50 %$WO_3/ZrO_2 + C_{act}$	20.7	25.0	33.1	7.4	5.3	0	3.0	11.1
13	36 %$WO_3/TiO_2 + C_{act}$	19.8	27.9	21.2	4.5	5.1	0	2.8	26.6
14	50 %$WO_3/Al_2O_3 + C_{act}$	21.2	27.7	40.9	4.7	1.5	0	0.3	3.0
15[e]	WO_3	100	48.9	7.4	0.9	1.7	0.7	0.8	6.8
16[e]	50 %$WO_3/Al_2O_3 + C_{act}$	100	16.6	30.7	1.8	0.2	0	0.4	0.6
17[e]	12 %WO_3/TiO_2	100	8.7	8.2	3.2	2.1	4.4	3.9	45.9
18	WO_2	20.6	41.4	8.1	1.3	2.8	0	0.7	12.6
19	W	13.0	31.4	8.0	6.8	2.3	0.3	1.7	15.6
20	W_2C	22.7	50.8	11.4	1.4	3.3	0.1	0.8	5.3

[a] 478 K, 6 MPa H_2, 30 min, 40 mL H_2O, 1.0 g cellulose, 0.02 g 3 wt% Ru/C. [b] 1.0 g for bulk WO_3, WO_2, W, and W_2C catalysts, 0.016 g WO_3 for supported WO_3 catalysts, and 1.0 g for activated carbon when used. [c] Erythritol and threitol. [d] Ribitol, arabitol, and xylitol. [e] 518 K, 6 MPa H_2, 30 min.

unchanged (22.8 % vs. 23.4 %), but instead of ethylene glycol, propylene glycol surprisingly became the major product with a selectivity of 31.9 % (Table 1, entry 3). The role of additional C_{act} was examined in the presence of Ru/C, and no contribution to the formation of propylene glycol was observed when WO_3 was absent (Table 1, entry 4). By supporting the WO_3 crystallites on C_{act} (e.g., 0.5 wt % WO_3), a similar result of 37.6 % propylene glycol selectivity was obtained at 20.1 % conversion (Table 1, entry 5), thus indicating that C_{act} and WO_3 work individually for the formation of propylene glycol without requirement of their close contact. Activated carbon appears to accelerate the isomerization of glucose into fructose by its surface basicity, as confirmed by a separate experiment of glucose isomerization on C_{act} (not shown here). Fructose is most likely the active intermediate for propylene glycol while glucose is the precursor for ethylene glycol on WO_3, as discussed below.

A parallel study showed that the catalytic property of WO_3 strongly depends on its domain size, which was varied by changing its surface density on different supports (e.g., ZrO_2, Al_2O_3, and TiO_2). When the surface density of WO_3 on ZrO_2 increased from 2.2 to 11.0 W nm^{-2}, especially from 4.2 to 6.4 W nm^{-2}, the selectivity to ethylene glycol increased sharply from 11.5 % to 34.9 %, while the selectivity to hexitols concurrently decreased from 63.4 % to 31.4 % (Figure 1 a). The conversion and selectivity to propylene glycol slightly varied from 18.5 to 20.1 % and from 4.0 to 6.5 %, respectively, in the whole range of surface density of WO_3. Similar trends were observed on other supports, such as Al_2O_3 and TiO_2 (Table 1, entries 6–11). Increase in the surface density of WO_3 on Al_2O_3 and TiO_2 in the range of approximately 2 to 7 W nm^{-2} led to an increase in the selectivity to ethylene glycol from 25.5 % to 45.0 % and 10.2 % to 37.5 %, respectively, with a concurrent decline in the selectivity to hexitols from 43.4 % to 16.8 % and 70.0 % to 29.7 %, respectively. These WO_3 domains were characterized by X-ray diffraction (XRD) analysis (Figure S1 in the Supporting Information) and Raman spectroscopy (Figure 1 b and Figure S2). These analyses showed that the domains evolve from dispersed mono- and polytungstates at WO_3 surface densities below approximately 5 W nm^{-2}, the theoretical monolayer capacity,[12] to three-dimensional WO_3 crystallites at WO_3 surface densities above approximately 5 W nm^{-2}. This correlation is represented by the Raman spectra of the WO_3/ZrO_2 samples (Figure 1 b), which show the characteristic features of crystalline WO_3 at about 807, 720, and 270 cm^{-1} above 5.3 W nm^{-2}. Such structural evolution is consistent with the general conclusions reported previously.[12] These parallel changes in the structure of the WO_3 domains and their selectivities show that the dispersed WO_3 species are active mainly as solid acid for the cellulose hydrolysis, while the WO_3 crystallites not only act as solid acid but also catalyze the cleavage of the C–C bonds in the sugar intermediates.

At given WO_3 surface densities especially below a coverage of one monolayer, it was noted that WO_3 supported on TiO_2 and ZrO_2 afforded higher selectivity to hexitols while conversion to ethylene glycol was preferred on Al_2O_3 (Table 1, entries 6–11). Such a support effect may be related to the different surface basicities of these supports and thus the different interactions with the sugar intermediates, as was inferred from the separate experiments with these pure supports (Table S1). Addition of C_{act} to the supported WO_3

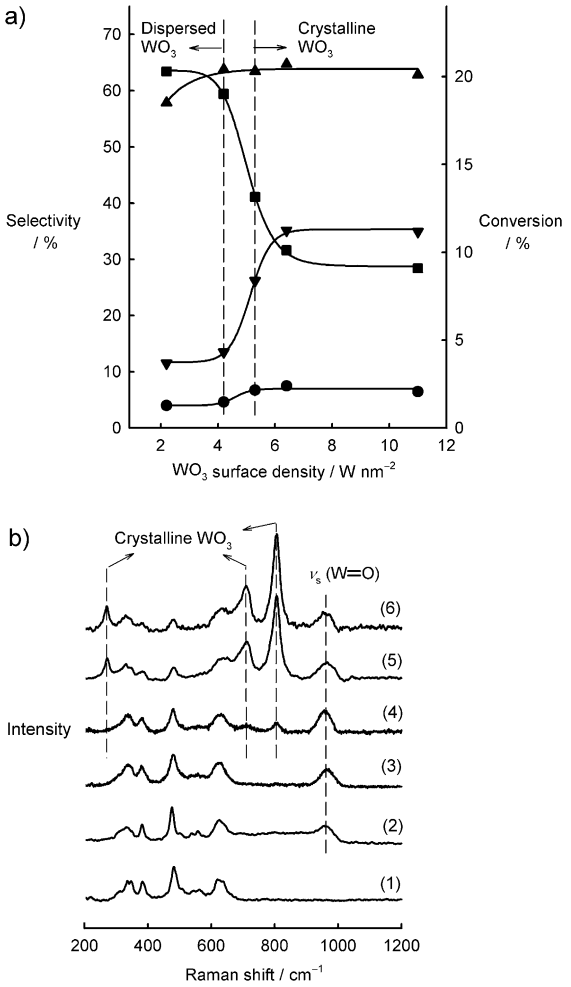

Figure 1. a) Cellulose conversion and product selectivity as a function of the surface density of WO_3 on ZrO_2 (478 K, 6 MPa H_2, 30 min, 40 mL H_2O, 1.0 g cellulose, 0.02 g 3 wt% Ru/C, 0.016 g WO_3). Left hand axis: selectivity for hexitols (■), for ethylene glycol (▼), for propylene glycol (●); right hand axis: cellulose conversion (▲). b) Raman spectra of ZrO_2 (1) and WO_3 on ZrO_2 with different WO_3 loadings and surface densities: 2) 12 wt% WO_3/ZrO_2 (2.2 W nm^{-2}), 3) 24 wt% WO_3/ZrO_2 (4.2 W nm^{-2}), 4) 30 wt% WO_3/ZrO_2 (5.3 W nm^{-2}), 5) 36 wt% WO_3/ZrO_2 (6.4 W nm^{-2}), 6) 50 wt% WO_3/ZrO_2 (11.0 W nm^{-2}).

samples, which dominantly consisted of WO_3 crystallites, also led to a change in product distributions (Table 1, entries 12–14), as observed with bulk WO_3 (Table 1, entries 2 and 3). For example, the selectivity to propylene glycol increased significantly from 10.0% to 40.9%, while the selectivity to ethylene glycol and to hexitols decreased from 45.0% to 27.7% and 16.8% to 3.3%, respectively, at a similar cellulose conversion (≈21%) after addition of C_{act} into 50 wt% WO_3/Al_2O_3 (7.2 W nm^{-2}). These results show that the synthesis of ethylene glycol, propylene glycol, and hexitols can be controlled by changing, for example, the domain size of WO_3 and the support.

The high selectivity toward these polyols can be retained even at 100% cellulose conversion on these WO_3 catalysts (Table 1, entries 15–17). For example, the selectivities to ethylene glycol, propylene glycol, and hexitols were 48.9%, 30.7%, and 49.8%, respectively, on bulk WO_3, 50 wt% WO_3/Al_2O_3 (7.2 W nm^{-2}) mixed with C_{act}, and 12wt% WO_3/TiO_2 (2.2 W nm^{-2}), respectively, corresponding to their respective yields at 100% conversion achieved at 518 K. To the best of our knowledge, such high yields, more specifically of propylene glycol (30.7%), have not been reported previously for the direct reaction of cellulose. Obviously, these yields can be potentially improved by optimizing the catalyst performance and reaction conditions.

The recyclability of these WO_3 catalysts was also examined. No essential decline in cellulose conversion and polyol distribution was observed after five successive cycles either on bulk WO_3 or 50wt% WO_3/Al_2O_3 (7.2 W nm^{-2}) mixed with C_{act} (representative results in Figure S3). Such stable performance of these WO_3 catalysts is consistent with their characterization results. Analysis of the aqueous reaction solutions by inductively coupled plasma atomic emission spectroscopy (ICP-AES) showed no detectable leaching of WO_3. Characterization by XRD analysis, Raman spectroscopy, and X-ray photoelectron spectroscopy (XPS) showed no change or modification in the bulk and surface of WO_3 and in its oxidation state after reactions (Figure S4–7). These results demonstrate that the bulk and supported WO_3 catalysts are stable and reusable under the reaction conditions in this work.

To confirm that WO_3 is the active phase for the cleavage of C–C bonds in the sugar intermediates, other tungsten samples were compared under identical conditions, including crystalline WO_2, W_2C, and W in different oxidation states. Similar to WO_3, WO_2, and W_2C catalyzed the cellulose reaction with 41.4% and 50.8% selectivity to ethylene glycol at 20.6% and 22.7% conversion, respectively (Table 1, entries 18–20). Even on tungsten powder, the selectivity to ethylene glycol was as high as 31.4% at 13.0% cellulose conversion. To understand the performances of these tungsten species, they were characterized by XPS, XRD analysis, and Raman spectroscopy. XPS spectra showed that as-received WO_2, W_2C, and W contained W^{VI} species at their surfaces with estimated molar fractions of 68%, 46%, and 54%, respectively (Figure S6). Such high surface contents of W^{VI} may be relevant to the preparation of these species, which involves either reduction of WO_3 (for WO_2 and W) or passivation in O_2 (for W_2C).[7a,13] Irrespective of this difference, the surfaces of these species were predominantly covered with the W^{VI} after the cellulose reaction, thus showing the intensive oxidation at their surfaces to WO_3 (Figure S6). This result is consistent with the detection of the WO_3 phase after the reaction by Raman spectroscopy (Figure S5), nevertheless, the bulk phases of these species remained essentially intact (Figure S4). In contrast, WO_3 was very robust and stable, as mentioned before. Such difference in their structural stability indicates that the WO_3 phase plays the key role in breaking the C–C bonds and forming ethylene glycol. Notwithstanding its superior activity and hydrothermal stability in the cellulose reaction, WO_3 possesses additional advantages over the other three tungsten samples, which are generally derived from WO_3, with respect to price and availability.

In order to understand the mechanism for the conversion of cellulose to ethylene glycol and propylene glycol involving

Table 2: Conversion and selectivity in reactions of different sugars and sorbitol on Ru/C.[a]

Entry		Selectivity [%]						
		Ethylene glycol	Propylene glycol	Glycerol	Tetritols[b]	Pentitols[c]	Mannitol	Sorbitol
		C_2	C_3	C_3	C_4	C_5	C_6	C_6
1	sorbitol + WO_3	0	0	0	0	0	0	100
2	glucose	9.3	6.1	1.9	0	3.5	7.4	70.3
3	fructose	8.3	6.6	2.9	0.3	1.9	35.8	43.5
4	glucose + WO_3	59.4	14.1	2.9	4.5	0	1.8	9.2
5	fructose + WO_3	15.7	47.9	17.7	1.0	0	9.4	10.8
6	mannose + WO_3	54.2	11.3	3.4	5.3	0	17.6	3.3
7	xylose + WO_3	32.1	35.5	10.0	5.3	15.5	–	–
8	ribose + WO_3	25.8	29.0	7.6	0.3	20.3	–	–
9[d]	2-deoxy-glucose + WO_3	0	0	0	0	0	0	0
10[e]	2-deoxy-ribose + WO_3	0	0	0	0	0	–	–

[a] 478 K, 10 min, 6 MPa H_2, 40 mL H_2O, 0.1 g sugar or sorbitol, 0.02 g 3 wt%Ru/C, 1.0 g WO_3; sorbitol conversion was 1.4% and sugar conversions are all 100%. [b] Erythritol and threitol. [c] Ribitol, arabitol, and xylitol. [d] The product is 2-deoxy-sorbitol. [e] The product is 2-deoxy-ribitol.

the C–C bond cleavage, reactions of the possible intermediates, glucose, fructose, and sorbitol, were performed on WO_3 under identical conditions (at 478 K and 6 MPa H_2). Sorbitol was found to be inactive with a negligible conversion (1.4%) after 10 minutes (Table 2). Glucose and fructose were readily reduced to sorbitol and to a mixture of sorbitol and mannitol, respectively, with nearly equimolar amounts on Ru/C without WO_3. In the presence of WO_3, glucose was converted to ethylene glycol in a selectivity of 59.4% (at 100% conversion) with a similar product distribution to that observed in the cellulose reaction. However, for the fructose reaction, C_3 polyols were formed dominantly, including 47.9% propylene glycol and 17.7% glycerol, as found in the cellulose reaction on WO_3 mixed with C_{act}. Reaction of mannose, an alternative isomer of glucose from the cellulose hydrolysis, was also examined on WO_3, which afforded ethylene glycol as the major product (54.2%), like the glucose reaction, but with an expected higher mannitol selectivity (17.6%) than sorbitol selectivity (3.3%). Therefore, glucose and fructose are the precursors of ethylene glycol and propylene glycol, respectively, which are formed through selective cleavage of the C–C bonds in these sugar molecules on WO_3 and subsequent hydrogenation of the corresponding degraded intermediates on Ru/C (Scheme 1).

These results of the C_6 sugar reactions indicate that the cleavage of the C–C bond occurs primarily at the β position to the carbonyl group. This is further verified by the reactions of C_5 sugars, xylose, and ribose, which form nearly equimolar amounts of ethylene glycol and C_3 polyols (propylene glycol and glycerol; Table 2, entries 7 and 8). Such a cleavage pattern resembles the pattern predicted by the retro-aldol mechanism, which has been used previously to understand the sugar hydrogenolysis reaction under basic conditions.[11a,14] However, this mechanism was excluded by reactions of 2-deoxy-glucose and 2-deoxy-ribose on WO_3 and Ru/C under the same conditions (Table 2, entries 9 and 10). If the reactions followed the retro-aldol mechanism, the major products would be ethylene glycol and ethanol for 2-deoxy-glucose, and propylene glycol and ethanol for 2-deoxy-ribose. But only their sugar alcohols, 2-deoxy-sorbitol and 2-deoxy-ribitol, were formed with no detectable products derived from the C–C bond cleavage in the two 2-deoxy-sugars. Taken together, these results demonstrate that the adjacent α-OH group (i.e., next to the carbonyl group) in the sugars is indispensable to undergo the C–C bond cleavage on WO_3, different from the typical retro-aldol reaction that requires the presence of only β-OH to the carbonyl groups. Detailed studies on the underlying reaction mechanism are in progress, however, we tentatively propose that the involved cleavage of the C–C bond in the cellulose reaction may proceed through complexation of the sugar intermediates with WO_3. The complexation probably involves the carbonyl oxygen atoms and three hydroxylic oxygen atoms at the α-, β-, and γ-OH groups of the sugars, and leads to the rearrangement of the C–C bonds of the sugars, as proposed by Hayes et al. for the epimerization of aldoses on molybdates.[15]

In conclusion, we have found that structurally stable and readily available WO_3 crystallite is efficient in the acceleration of the hydrolysis of cellulose to sugar intermediates, and more significantly in the selective cleavage of the C–C bonds in these sugars. In combination with the hydrogenation step on Ru/C, this approach leads to the controllable synthesis of ethylene glycol, propylene glycol, and sorbitol from cellulose. Further studies on the fine design of WO_3 structures and catalysts that are effective for the isomerization of glucose into fructose, together with optimization of the two competitive reactions of the sugar hydrogenation and degradation, will improve the yields and productivity of ethylene glycol and propylene glycol with promising potential for industrial purposes.

Experimental Section

Ru/C catalysts were prepared by incipient wetness impregnation of activated carbon (AR, Beijing Dali Fine Chemical) with an aqueous solution of $RuCl_3$ (GR, Sinopharm Chemical), followed by drying at 383 K in air and reduction at 623 K in a 20% H_2 in N_2 flow. Supported WO_3 catalysts were prepared by incipient wetness impregnation of different supports, including activated carbon, ZrO_2, TiO_2, and Al_2O_3, with aqueous solutions of ammonium metatungstate (AR, Sinopharm Chemical), subsequent drying at 383 K in air, and calcination at 773 K in an air flow (except WO_3/C, which was calcinated in a N_2 flow). Bulk WO_3 was purchased from Beijng Chemical Works (>99.0%), bulk

WO_2 (99.9%) and W_2C (99.5%) from Alfa Aesar, and bulk W (>99.8%) from Sinopharm Chemical.

XPS spectra were obtained on Kratos Axis Ultra with Al Kα source ($h\nu = 1486.7$ eV) and a hemispherical electron analyzer connected to an eight-channel detector. The C1s line at 284.8 eV was used as an internal standard for binding-energy correction. XRD patterns were taken on a Rigaku D/MAX-2400 diffractometer using Cu Kα1 radiation ($\lambda = 1.5406$ Å) operated at 40 kV and 100 mA. Raman spectra were collected in ambient conditions with a resolution of 1.5 cm^{-1} on Renishaw 1000 micro-Raman spectroscopy using a 632.8 nm He–Ne laser. BET surface areas were measured by nitrogen physisorption at its normal boiling point on an ASAP 2000 analyzer. WO_3 surface densities ($W\,nm^{-2}$) of the supported catalysts were estimated from the WO_3 contents and BET surface areas.

Cellulose (Alfa Aesar, microcrystalline) reactions were carried out in water (40 mL) in a stainless autoclave (total volume 100 mL) typically at 478 K and 6 MPa H_2 for 30 min with vigorous agitation. Products in liquid solutions were analyzed by HPLC analysis (Shimadzu LC-20A), and in gaseous phase by GC analysis (Shimadzu 2010GC). Cellulose conversion was determined by the weight difference of cellulose before and after the reaction; product selectivities were calculated on the carbon basis.

Received: January 13, 2012
Published online: February 24, 2012

Keywords: cellulose · glycols · heterogeneous catalysis · hydrolysis · tungsten trioxide

[1] G. W. Huber, S. Iborra, A. Corma, *Chem. Rev.* **2006**, *106*, 4044–4098.

[2] a) P. Gallezot, *Catal. Today* **2007**, *121*, 76–91; b) D. Klemm, B. Heublein, H. Fink, A. Bohn, *Angew. Chem.* **2005**, *117*, 3422–3458; *Angew. Chem. Int. Ed.* **2005**, *44*, 3358–3393.

[3] S. van de Vyver, J. Geboers, P. A. Jacobs, B. F. Sels, *ChemCatChem* **2011**, *3*, 82–94.

[4] a) R. Rinaldi, F. Schüth, *ChemSusChem* **2009**, *2*, 1096–1107; b) Y. S, H. M. Brown, X. Huang, X. Zhou, J. E. Amonette, Z. C. Zhang, *Appl. Catal. A* **2009**, *361*, 117–122; c) A. Onda, T. Ochi, K. Yanagisawa, *Green Chem.* **2008**, *10*, 1033–1037; d) J. M. Robinson, C. E. Bungess, M. A. Bently, C. D. Brasher, B. O. Horre, D. M. Lillard, J. M. Macias, H. D. Mandal, S. C. Mills, K. D. O'Harra, J. T. Pon, A. F. Raigoza, E. H. Sanchez, J. S. Villarreal, *Biomass Bioenergy* **2004**, *26*, 473–483; e) M. Sasaki, Z. Fang, Y. Fukushima, T. Adschiri, K. Arai, *Ind. Eng. Chem. Res.* **2000**, *39*, 2883–2890; f) J. Geboers, S. Van de Vyver, K. Carpentier, K. de Blochouse, P. Jacobs, B. Sels, *Chem. Commun.* **2010**, *46*, 3577–3579; g) R. Palkovits, K. Tajvidi, A. M. Ruppert, J. Procelewska, *Chem. Commun.* **2011**, *47*, 576–578; h) J. Geboers, S. Van de Vyver, K. Carpentier, P. Jacobs, B. Sels, *Chem. Commun.* **2011**, *47*, 5590–5592.

[5] a) A. Fukuoka, P. L. Dhepe, *Angew. Chem.* **2006**, *118*, 5285–5287; *Angew. Chem. Int. Ed.* **2006**, *45*, 5161–5163; b) P. L. Dhepe, A. Fukuoka, *ChemSusChem* **2008**, *1*, 969–975; c) H. Kobayashi, T. Komanoya, K. Hara, A. Fukuoka, *ChemSusChem* **2010**, *3*, 440–443.

[6] a) C. Luo, S. Wang, H. Liu, *Angew. Chem.* **2007**, *119*, 7780–7783; *Angew. Chem. Int. Ed.* **2007**, *46*, 7636–7639; b) T. Deng, J. Sun, H. Liu, *Sci. China Ser. B* **2010**, *53*, 1476–1480; c) N. Yan, C. Zhao, C. Luo, P. J. Dyson, H. Liu, Y. Kou, *J. Am. Chem. Soc.* **2006**, *128*, 8714–8715.

[7] a) N. Ji, T. Zhang, M. Zheng, A. Wang, H. Wang, X. Wang, J. G. Chen, *Angew. Chem.* **2008**, *120*, 8638–8641; *Angew. Chem. Int. Ed.* **2008**, *47*, 8510–8513; b) N. Ji, T. Zhang, M. Zheng, A. Wang, H. Wang, X. Wang, Y. Shu, A. L. Stottlemyer, J. G. Chen, *Catal. Today* **2009**, *147*, 77–85; c) L. Ding, A. Wang, M. Zheng, T. Zhang, *ChemSusChem* **2010**, *3*, 818–821.

[8] a) W. Deng, X. Tan, W. Fang, Q. Zhang, Y. Wang, *Catal. Lett.* **2009**, *133*, 167–174; b) W. Deng, M. Liu, Q. Zhang, X. Tan, Y. Wang, *Chem. Commun.* **2010**, *46*, 2668–2670.

[9] S. van de Vyver, J. Geboers, M. Dusselier, H. Schepers, T. Vosch, L. Zhang, G. Van Tendeloo, P. A. Jacobs, B. F. Sels, *ChemSusChem* **2010**, *3*, 698–701.

[10] a) R. D. Cortright, R. R. Davda, J. A. Dumesic, *Nature* **2002**, *418*, 964–967; b) J. N. Chheda, G. W. Huber, J. A. Dumesic, *Angew. Chem.* **2007**, *119*, 7298–7318; *Angew. Chem. Int. Ed.* **2007**, *46*, 7164–7183.

[11] a) J. Sun, H. Liu, *Green Chem.* **2011**, *13*, 135–142; b) S. Wang, Y. Zhang, H. Liu, *Chem. Asian J.* **2010**, *5*, 1100–1111; c) S. Carrettin, P. McMorn, P. Johnston, K. Griffin, C. J. Kiely, G. A. Attand, G. J. Hutchings, *Top. Catal.* **2004**, *27*, 131–136.

[12] a) D. G. Barton, M. Shtein, R. D. Wilson, S. L. Soled, E. Iglesia, *J. Phys. Chem. B* **1999**, *103*, 630–640; b) J. Macht, C. D. Baertsch, M. May-Lozano, S. L. Soled, Y. Wang, E. Iglesia, *J. Catal.* **2004**, *227*, 479–491; c) I. E. Wachs, T. Kim, E. I. Ross, *Catal. Today* **2006**, *116*, 162–168.

[13] S. Ramanathan, S. T. Oyama, *J. Phys. Chem.* **1995**, *99*, 16365–16372.

[14] K. Y. Wang, M. C. Hawley, D. D. Furney, *Ind. Eng. Chem. Res.* **1995**, *34*, 3766–3770.

[15] M. L. Hayes, N. J. Pennings, A. S. Serianni, R. Barker, *J. Am. Chem. Soc.* **1982**, *104*, 6764–6769.

